

The Three-Dimensional Elemental Distribution of 3D Printing Stainless Steel Gear via Confocal 3D-XRF Analysis

Min Qin¹, Longtao Yi², Jingbang Wang¹, Yue Han¹, Tianxi Sun¹, Zhiguo Liu¹

¹The Key Laboratory of Beam Technology and Material Modification of the Ministry of Education, Beijing Normal University, Beijing 100875, China

²The Institute of Nuclear Physics and Chemistry, China Academy of Engineering Physics, Mianyang 621000, China

Abstract. The macroscopic mechanical properties of 3D printing product are closely related to their microstructure, it has significant importance to accurately characterize the micro-structure of 3D printing products. Confocal three-dimensional micro-X-ray fluorescence (3D-XRF) is a good surface analysis technology widely used to analyse elements and elemental distributions. Therefore, this technique is also very suitable for element distribution measurement of 3D printing product which is printed layer by layer. In this paper the 3D-XRF technique was used to study the spatial elemental distribution of a micro zone from the 3D printing stainless steel gear. An elemental mapping of two orthogonal sections in the depth direction and three dimensional elemental rendering of one micro-region were obtained. The result shows that elemental distribution of the sample is not uniform, the elemental layer structure is formed in the depth direction, the content of the element in measured area vary smoothly, and with no elemental mutation region. This indicates that the 3D printing sample are fused well between layers and layers, with no large pores or bubbles inside the sample. This study demonstrates that it is feasible to make assessment for micro-structure of 3D printing metal product by using confocal 3D-XRF.

1. Introduction

3D printing is one of rapid prototyping technologies with the characteristic of manufacturing layer by layer [1]. Because the macroscopic mechanical properties of 3D printing products are closely related to their microstructure, it has significant importance to accurately characterize the micro-structure of 3D printing products in order to improve the performance and quality of 3D printing products. Currently, many research institutes has carried out many study works about characterization of micro-structure of 3D printing product [2-4], mainly using some of the traditional characterization methods, such as density detection, morphology analysis and phase analysis [5, 6]. The latest report concerning the characterization of 3D printing metal sample is that ROSS CUNNINGHAM et al. [7] obtained the synchrotron XCT rendering of 3D printing Ti-6Al-4V alloy sample by using the synchrotron X-ray microtomography in 2016. The traditional characterization methods e.g. Electron spectroscopy can only get the surface elemental distribution, and the sample need to be destructively prepared. Although the synchrotron XCT technique has higher resolution and analysis depth, but it is too expensive and hard to apply for test time. The 3D-XRF is a non-destructive technique, easy to implement in general laboratory. What's more, the spatial elemental distribution can be obtained non-destructively by the confocal 3D-XRF.

Confocal three-dimensional micro X-ray fluorescence (3D-XRF) based on the polycapillary X-ray lenses is an excellent surface analysis technology. It has been widely used in the biological science,



material science, environmental science, archaeology etc. [8-13], since Gibson and Kumakhov [14] proposed the principle of 3D-XRF combined with the use of two individual polycapillary X-ray lenses in 1993. By using polycapillary X-ray lenses in both the excitation and detection channels, a confocal volume could be obtained. Because the polycapillary X-ray lens limits the viewing area of the detector, radiation were shielded from the detector. Therefore only radiation from the confocal volume could be detected. If the sample is moved through this micro-volume, the space information about elementary composition of the sample can be obtained. Based on the above principles, it is possible to perform 3D elemental mapping non-destructively using this method. It is also an ideal method to analyse samples with lamellar structure. So it is suitable to make spatial elemental distribution analysis of 3D printing sample by confocal 3D-XRF. By analyzing the distribution of elements in the micro-region of the sample, it is possible to make an assessment to fusion situation of interlayer inside 3D printing products, such as whether exists pores or bubbles.

In this work the 3D-XRF technique was used to study the spatial elemental distribution of a micro region from the 3D printing stainless steel gear. An elemental mapping of two orthogonal sections in the depth direction and three dimensional elemental rendering of a micro-region were obtained by using a tabletop confocal 3D-XRF set-up in laboratory. Based on the results, the microstructure of the 3D printing stainless steel gear can be evaluated.

2. Experimental

2.1. Confocal 3D-XRF set-up

Figure 1 (b) shows the confocal 3D XRF setup. An X-ray tube with a Mo target (XTG UltraBright Microfocus X-ray Source, Oxford, USA) was operated at 20kV and 0.5mA. The focal spot size of the X-ray tube was $16.45\mu\text{m}$ at 20kV. The polycapillary full X-ray lens (PFXRL) for X-ray irradiation was attached to the X-ray tube, and a polycapillary parallel X-ray lens (PPXRL) was attached to a silicon drift detector (X-123, AMPtek, USA). Each polycapillary lens was designed and manufactured by the Key Laboratory of Beam Technology and Material Modification of the Ministry of Education, Beijing Normal University. The input focal distance and output focal distance of the full lens was 52.9mm and 11.5mm, respectively. The focal distance of the half lens was 14.9mm. The sizes of the focal spot of the half lens and full lens were experimentally determined to be $33\mu\text{m}$ and $32.4\mu\text{m}$ at 17.4keV (Mo Ka), respectively. Both polycapillary X-ray lenses were positioned in the confocal geometry, as shown in figure 1 (a). The micro volume overlaps the output focal spot of the PFXRL and the input focal spot of the PPXRL. The angle between the incident and detection beams was set to 90° .

The depth resolution is $47\mu\text{m}$ at 7.4 keV (Ni Ka). The sample stage was installed on an X-Y-Z stage [DS102 Series, SURUGA SEIKI, Japan], and the corresponding step resolution was $0.5\mu\text{m}$ of each axis. A CCD camera was also used to confirm the relative position between the sample and confocal volume.

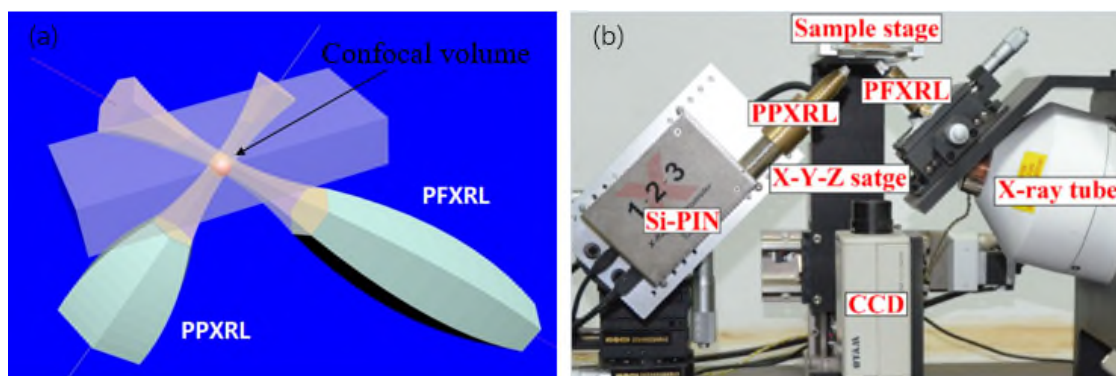


Figure 1 (a) Schematic diagram of the confocal geometry
(b) Experimental setup of the confocal 3D-XRF.

2.2. Sample

Figure 2 shows the photographs of the 3D printing metal gear whose material is 316L stainless steel. It was printed by 3D systems Company, with the thickness of printing layer is about $20\mu\text{m}$. To study the spatial distribution of the sample, a series of elemental mapping analysis based on the confocal 3D-XRF technique were applied to the region (R) and region (C). The micro-region (R) is a $1000\times 700\times 40\mu\text{m}$ small cuboid, as shown in figure 2 (c). As shown in figure 2 (d), the micro-region (C) is two orthogonal sections in the depth direction, with the area dimension is $600\times 184\mu\text{m}$.

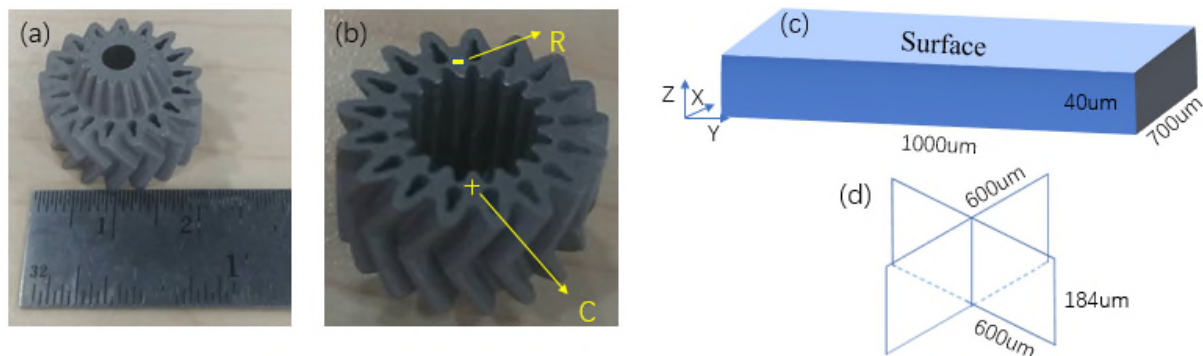


Figure 2. Photographs of the 3D printing stainless steel gear (a) the size of sample (b) schematic diagram of measurement region (c) the size of measurement R-region (d) the size of measurement C-region.

3. Result and discussion

3.1. Elemental components

To ensure the main elemental composition of the sample in this study, a confocal 3D-XRF was applied to this 3D printing stainless steel gear, with the measurement time is 45s. As shown in figure 3, Cr, Mn, Fe, and Ni were detected. This detection results are consistent with the main metal elements contained in 316L stainless steel.

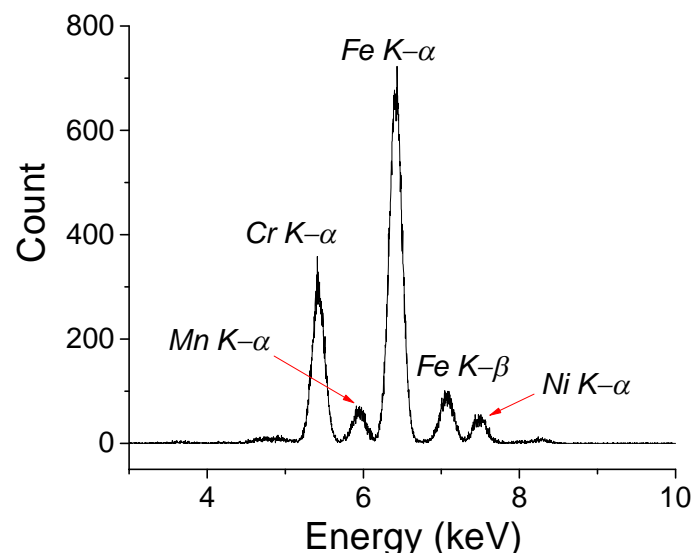


Figure 3. Fluorescence spectra of the 3D printing stainless steel gear.

3.2. Elemental mapping in depth direction

Figure 4 shows the elemental mapping of two orthogonal sections in depth direction of region C with an analysis depth of $184\mu\text{m}$. The dimensions of two sections are the same. As shown in figure 5 that the content of 4 elements in measured area vary smoothly, and with no elemental mutation region. It

can be observed from the enlarge figures that the fluorescence counting strength of three elements in terms of Cr, Fe and Mn increase first, then decrease, and then increase again. These trends indicates that the elemental distribution isn't uniform and the elemental layer structure is formed in the depth direction inside the 3D printing sample.

It can be inferred from figure 4 that the 3D printing sample is fused well between layers and layers, with no large pores or bubbles. But the elemental layer structure is formed along the depth direction, perhaps because of the layer and layer forming method.

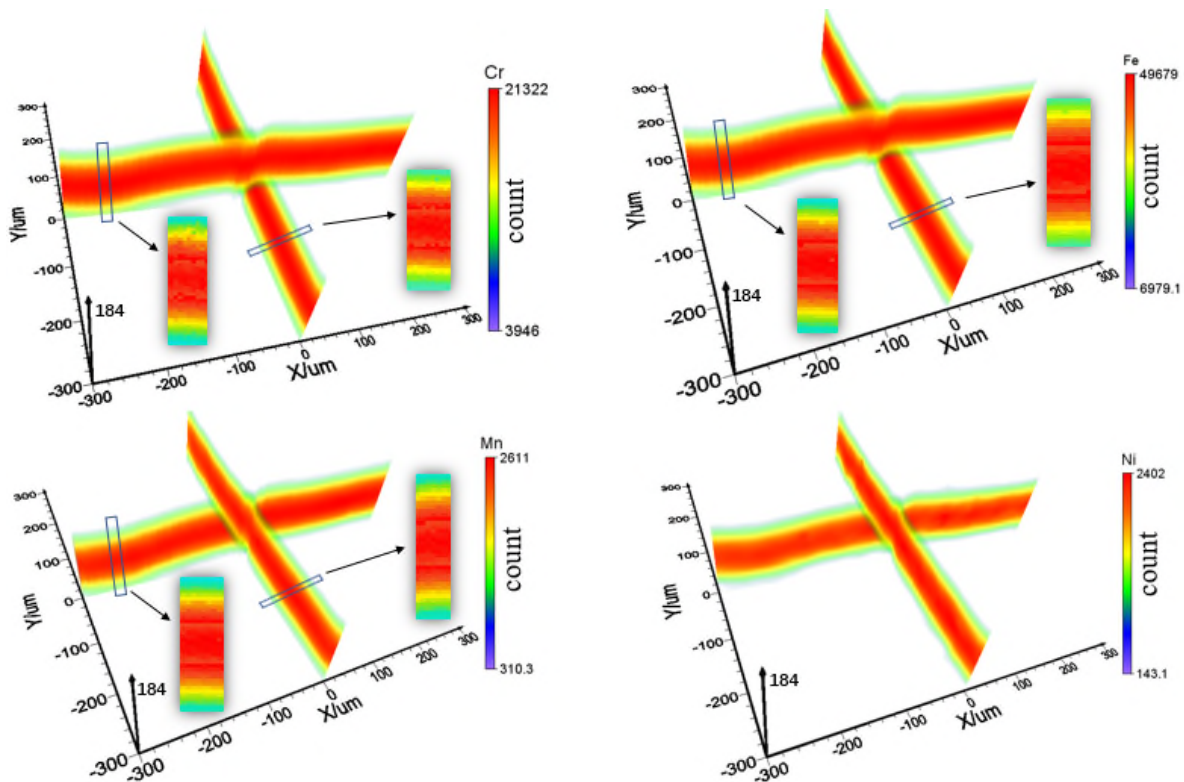


Figure 4. Two orthogonal sections' elemental mapping of Cr, Fe, Mn, Ni in the region of C measured by confocal 3D-XRF set-up.

3.3. Three-dimensional elemental rendering

To confirm the 3D elemental distributions in the region R, a series of 3D elemental mapping analyses were performed at different depths. The scan depth range was from 0 to 40 μm , and the step was 10 μm . To more vividly show the spatial distributions of the elements in the sample, background intensity was wiped out from the 3D rendering.

As shown in figure 5, the spatial distributions of 4 elements are not uniform, respectively. The elemental distribution trends of Cr and Fe are consistent with the distribution trends of Ni and Mn. The content of Cr and Fe element was higher than the content of Ni and Mn in sample. It can be inferred that this elemental nonuniformity is caused by the uneven mixing of printing powder material or the insufficient elements diffusion during the printing process. Additionally, the content of 4 elements in measured volume vary smoothly, and with no elemental mutation region. So it indicates that the 3D printing sample is fused well between layers and layers inside that measured micro region, with no large pores or bubbles.

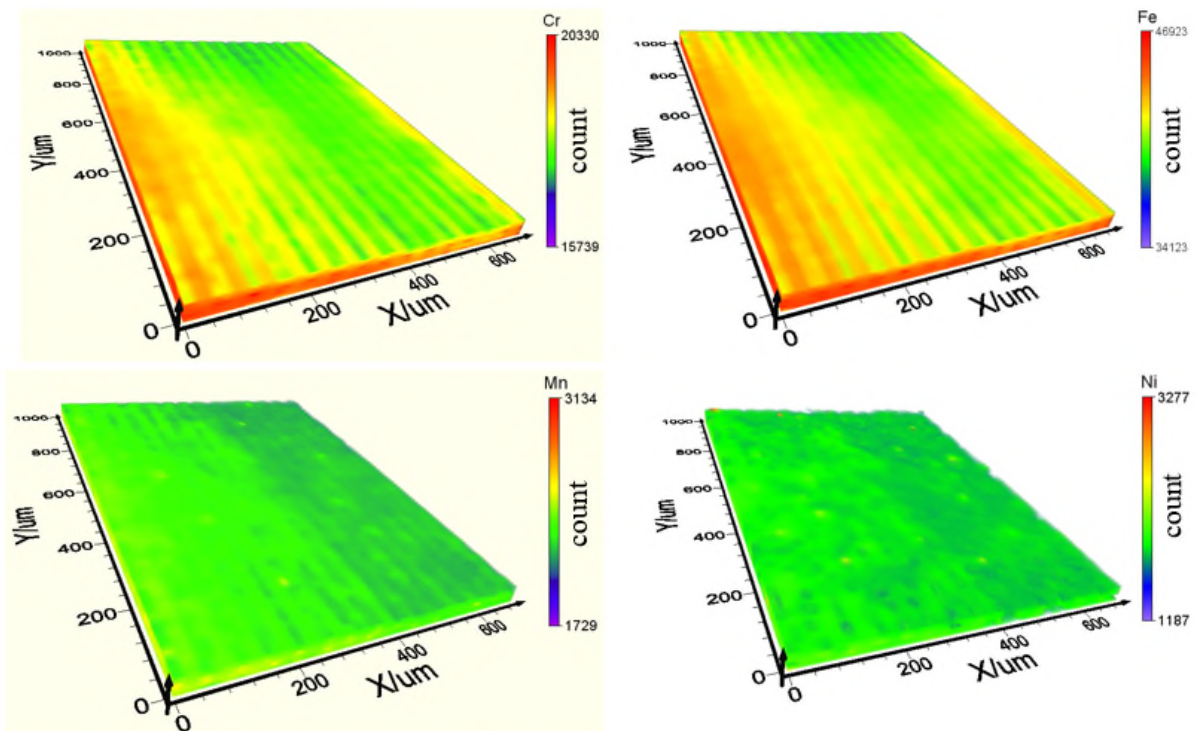


Figure 5. Three dimensional rendering of Cr, Fe, Mn, Ni in region of R measured by confocal 3D-XRF set-up.

4. Conclusion

We have firstly applied the confocal 3D-XRF technique to study the spatial elemental distribution of a 3D printing stainless steel gear. An elemental mapping of two orthogonal sections and three dimensional elemental rendering of one micro-region were obtained.

The results show that elemental distribution of the sample is not uniform, the elemental layer structure is formed in the depth direction, the content of the elements in measured region changes smoothly, and with no elemental mutation region. It can be inferred that this elemental non-uniformity is caused by the uneven mixing of printing powder material or the insufficient elements diffusion during the printing process. The results also indicate the 3D printing sample are fused well between layers and layers inside measured micro region, with no large pores or bubbles.

Hence, it is feasible to make assessment for micro-structure of 3D printing metal product by using confocal 3D-XRF. This method is a good supplement to the traditional characterization methods of 3D printing product.

References

- [1] Parthasarathya J and Starly B, 2010 *J. Mech. Behav. Biomed. Mater.* **3** 249-59.
- [2] Amato K N and Gaytan S M 2012 *Acta Mater.* **60** 2229-39.
- [3] Heintl P and Muller L 2008 *Acta Biomater.* **4** 1536-44.
- [4] Ramirez D A and Murr L E 2011 *Acta Mater.* **59** 4088-99.
- [5] Yadroitsev I and Bertrand Ph 2007 *Appl. Surf. Sci.* **253** 8064-9.
- [6] Gu D D and Shen Y F 2008 *Appl. Surf. Sci.* **255** 1880-7.
- [7] Cunningham R and Narra S P 2016 *Min. Met. Mater. Soc.* **68** 765-70.
- [8] West M and Ellis A T 2013 *J. Anal. At. Spectrom.* **28** 1544-90.
- [9] Šmit Z, Janssens K, Proost K and Langus I 2004 *Nucl. Instrum. Meth. B* **219** 35-40.
- [10] Woll A R, *Appl. Phys. A Mater. Sci. Process.* **83** 235-8.
- [11] Sun T and Liu H 2014 *Nucl. Instrum. Meth. B* **323** 25-9.
- [12] Kanngießer B and Malzer W 2012 *Appl. Phys. A Mater. Sci. Proc.* **106** 325-38.
- [13] Yi L T and Qin M 2016 *Appl. Phys. A.* **122** 856.

[14] Gibson W M and Kumakhov M A, *Int. Soc. Opt. Photonics* **9**.

Acknowledgments

This research was supported by National Natural Science Foundation of China (11675019). The 3D Print stainless steel gear was provided by 3D systems Company.